2024 European Control Conference (ECC)
June 25-28, 2024. Stockholm, Sweden

Implementation and validation of simultaneous state and parameter moving horizon estimation of a pressurized water reactor

Lucas Gruss[1, 2], Mohamed Yagoubi[1], Maxime Thieffry[1], Philippe Chevrel[1], and Alain Grossetête[2]

[1]LS2N (UMR 6004), IMT-Atlantique, 4 rue Alfred Kastler 44307 Nantes, France
[2]Reactor Process Department, Framatome, 1 pl. Jean Millet 92400 Courbevoie, France

***Abstract*— This paper presents the implementation of a Moving Horizon Estimation (MHE) approach for the simultaneous estimation of state and parameters within Pressurized Water Reactors (PWR) used in Nuclear Power Plants (NPPs). Addressing the inherent model stiffness, we leverage collocation as the integration method, making direct collocation a natural choice for transcription of the optimization problem into a nonlinear programming problem (NLP). The implementation benefits from state-of-the-art tools for modeling, expressing, and solving optimization problems, specifically CasADI and IPOPT. In a comparative analysis with a standard Extended Kalman Filter (EKF), our proposed MHE method exhibits superior performance and accuracy, even with rather classical tuning parameters.**

I. Introduction

A. Context

The need for cleaner energy drives the demand of renewable and nuclear alternatives in order to replace carbon-based energy. Gas and coal power plants are dispatchable sources of energy: they can quickly balance energy demand and offer on an electrical grid. Renewable sources of energy are intermittent as their output vary with the wheather. Hence, the burden of flexibility falls on nuclear power plants (NPP). This work focuses on pressurized water reactors (PWR), which make up the majority of nuclear reactors in the world.

Aging facilities across the globe, whose lifespan is poised to get extended, were not always designed with flexibility in mind. At the same time, numerous new NPP projects and designs such as EPR2 are in the works. Compliance with increasingly tighter safety demands and flexibility requirements of older and newer plants calls for accurate, reliable and possibly new monitoring and control solutions. These new approaches must be very carefully assessed, should they replace the existing, tried and studied methods already in use.

B. Problem statement

Authors in [1], [2] explore control of the core using Model Predictive Control (MPC) which was shown to outperform some of the most recent control strategies for core control, such as T mode. In MPC, a model of the controlled process is used to simulate the behaviour of the system over a window of time, over which optimal control actions are determined by repeatedly solving an optimal control problem (OCP). Requirements on performance, actuator constraints, system operating range and even economic operation of the plant can be met through the formulation of a constrained OCP. Despite its computational heaviness, capable hardware and software for MPC have contributed to the growing popularity of the methodology. However, control performance is heavily dependant on the accuracy of the model and knowledge of the system's state. In many practical applications, the state of the system is not readily available and model-plant mismatch must be adressed.

We consider the case where model-plant mismatch originates from parameter uncertainty in the model : modeling hypotheses and simplification can lead to model parameters that do not always match reality. A model can be calibrated for a specific operating point, though time-varying parameters still induce growing model-plant mismatch. Examples include: wear and tear or failure of moving parts, depletion and aging of consumable resources such as fuel, lubricant or catalizer.

For our use case, nuclear fuel is depleted and fission products accumulate throughout the fuel cycles. The cycles last about 18 months during which the dynamics involved in the core changes slowly. Such changes should be taken into account in the model in order to produce accurate state estimates and ensure the accuracy of the prediction model.

In this work, we present an extension to the work presented in [3], in which a moving horizon state estimator was proposed for a PWR. While its sensitivity to parameter uncertainty was assessed, we shall extend the algorithm to estimate parameters of interest of the model in order to improve the accuracy of both the state estimates and internal model used by the predictive controller [4]. The challenge lies in that the resulting optimization problem becomes harder to solve due to additional nonlinearities and decision variables.

C. Related works and contribution

The problem of estimating state and/or model parameters for NPP has been studied at length by the nuclear physics community. Even though plant designs and technologies differ across manufacturers, they are all governed by similar underlying principles. EKF [5] or neural networks [6] have been utilized for state estimation of a *point model*, a very simplified representation of the reactor's overall behavior without considering spatial details. This renders them less suitable for control dealing with axial phenomena. On the other side, in [7], [8], data assimilation (DA) techniques (a term coined by the meteorology community) may be employed to estimate xenon/iodine dynamics on an axial

model consisting of 30 nodes. Although the link is not made in the litterature, certain DA techniques applied to nuclear cores (such as 3D-var and 4D-var) are closely related to MHE and EKF methods. However, the complexity of this model results in a computational burden that is too significant for online use. In this study, we adopt a parsimonious model that is well-suited for control purposes, while still ensuring the desired online performance for an MPC or MHE scheme.

II. Modeling of a pressurized water reactor

Nuclear disintegration of a *fissile* nucleus can be achieved by collision with a neutron[9]. Its fission produces neutrons that can in turn induce the fission of other neighboring nuclei[10]. An NPP is a *heat machine*, whose heat source is as sustained chain reaction heating up the fuel and water in a pressurized tank. At the interface between the primary (core) and secondary circuits, steam generators produce steam driving the shaft of a power generator.

Cross-section of an isotope relates the kinetic energy of an incoming neutron with its probability of being involved in a nuclear reaction with the isotope. There is a cross-section for each type of nuclear reaction. The most common isotope in nuclear fuel is ^{235}U which is fissile under collision with a *thermal neutron*. Neutrons produced in fission of ^{235}U are in general too fast to cause the fission of other ^{235}U nuclei and need to be slowed down. The *moderator* slows neutrons when they bounce off of it, down to speeds more likely to cause fission. In PWR water is both the heat-transfer fluid and moderator. Moderation decreases as temperature of the water increases -due to a decreased density- which is called the *moderator effect*. The *doppler effect* describes the impact of the kinetic energy of the fuel on the probability of fission. ^{135}Xe is a crucial fission product to monitor; it is the main neutron poison in a nuclear core due to its very large cross-section in the thermal range.

Control of a nuclear core is achieved through the position of neutron-absorbant rods and the concentration of boron in the primary circuit's water. The controlled variable include temperature of the water, power distribution through the *axial offset* (AO). If we denote P_{top} and P_{bottom} the nuclear power produced in the top and bottom halves of the core, then we write:

$$AO = \frac{P_{\text{top}} - P_{\text{bottom}}}{P_{\text{top}} + P_{\text{bottom}}}$$

Modeling the behaviour of a core involves the coupling of the following physics phenomena:

- diffusion of the neutrons in the core.
- production of delayed neutrons.
- heating up of the fuel due to the nuclear reactions.
- heat exchange between the fuel and water.
- xenon poisoning.
- control actions: rods position, turbine power, boron concentration.
- moderator effect.
- doppler effect.

State of the art simulation codes use various methods to model these phenomena in each point of the system, such as Monte Carlo[11] and deterministic methods. Such models are not suitable for predictive control and monitoring due to their complexity. Instead of a 3D modelization of the core, we only consider a 1D axial representation which is essential to reconstruct the axial offset. The resulting model is described by a set of ordinary and partial differential equations. The system (see figure 1) is then discretized into 6 meshes comprising each a xenon concentration X_i, an iodine concentration I_i, a neutron density n_i and a delayed neutron density c_i, $i = 1..6$. T_i is the temperature at the interface between meshes i and $i+1$, $i = 2..6$ with T_1 being the temperature of water when entering the core, T_7 on exit. The boron concentration in the primary circuit C_b is introduced. The resulting model admits a state-space representation of the form:

$$\begin{aligned} \forall t \in \mathbb{R}, \quad & \dot{\mathbf{x}}(t) = f(t, \mathbf{u}(t), \mathbf{x}(t), \mathbf{p}), \quad \mathbf{x}(t) \in \mathbb{R}^{35}, \quad \mathbf{u}(t) \in \mathbb{R}^3 \\ & \mathbf{y}(t) = h(t, \mathbf{u}(t), \mathbf{x}(t), \mathbf{p}), \quad \mathbf{y}(t) \in \mathbb{R}^8, \quad \mathbf{p} \in \mathbb{R}^{m_p} \end{aligned}$$

$\mathbf{x}$ is the state of the system outlined above; $\mathbf{u}$ is the input to the system or signals that we take as input information which comprises the position of the control rods h_{rods}, boron concentration C_b and power of the turbine P_{turb}; $\mathbf{y}$ contains the available measurements from the system, i.e. neutron densities n_i and cold and hot leg temperatures T_{CL} and T_{HL}; $\mathbf{p}$ contains modelization parameters that influence the behaviour of the model and for which the estimation is of a particular interest. m_p is the number of estimated parameters.

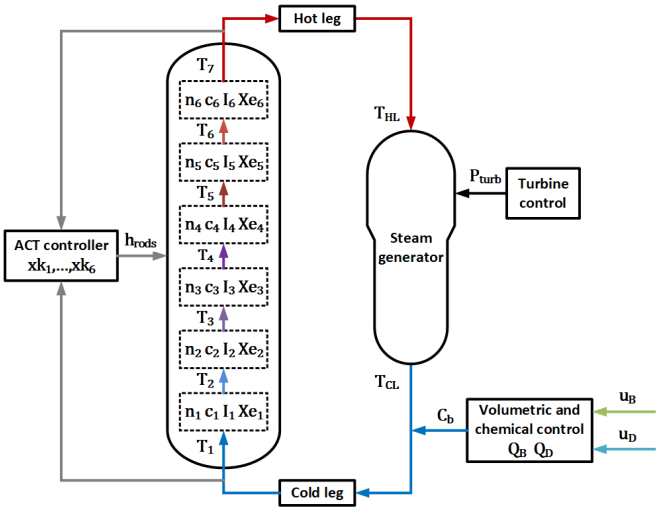

Fig. 1: Simplified view of a nuclear core.

The spatial discretization of the neutron diffusion equation leads to the introduction of an important parameter: the neutron exchange rate between node D. Instead of solving the transport equation, we consider that a constant share of the neutrons produced in each mesh makes its way to the neighboring meshes. This parameter summarizes more complex interactions in the fuel. The dynamics of the n_i can be summarized as:

$$\begin{aligned} \dot{n}_1 &= f_1(n_1, n_2, c_1, \rho_1, D) \\ \dot{n}_i &= f_i(n_{i-1}, n_i, n_{i+i}, c_i, \rho_i, D) \\ \dot{n}_6 &= f_6(n_5, n_6, c_6, \rho_6, D) \end{aligned}$$

where denotes ρ_i the localized anti-reactivity and depends

on the isotopic distribution and population, which evolve during normal operation and over the course of the fuel cycle. It is currently identified on state of the art neutronics codes at specific moments of the fuel cycle.

In addition, the xenon/iodine dynamics of the model writes $\forall i = 1, .., 6$:

$$\dot{X}_i = \lambda_I I_i - \lambda_X X_i + \Gamma_X n_i - \Sigma_X n_i X_i$$
$$\dot{I}_i = \Gamma_I n_i - \lambda_I I_i$$

Where λ_I and λ_X are the disintegration constants of ^{135}I and ^{135}Xe, Σ_X approximates the absorption cross-section of ^{135}Xe, Γ_X is the yield of the direct production of ^{135}Xe from the decay of the fuel and Γ_I is the yielf of production of iodine.

We assume a one group hypothesis, which considers all neutrons to have the same kinetic energy. As fission products accumulate, the kinetic energy spectrum of neutrons is changed and Σ_X should reflect this phenomenon.

The physics phenomena that need to be modeled in order to predict the behavior of a nuclear core have different time-scales. The main neutron poison ^{135}Xe has a half-life of 9.2 hours while the time-scales associated with fuel fission are of order of magnitude 10^{-5}s. As a result, the model is a stiff system of ordinary differential equations and appropriate techniques should be used in order to solve it numerically. Moreover, some of the dynamics of the model rely on interpolation tables obtained from highly precise neutronics codes. As a result the model performs better on operating ranges that are close to the setpoints at which the model was calibrated.

III. Moving horizon estimation

MHE is the dual estimation technique to MPC[12]. In MHE, granted detectability of the model, an optimization problem is solved repeatedly in order to estimate both states and model parameters. The algorithm uses past measurements $\mathbf{y}_{[t-H,t]}$ and past inputs $\mathbf{u}_{[t-H,t]}$ on the system over the finite-sized window $[t-H, t]$ of duration H. At each time instant t, state estimates over the window $\hat{\mathbf{x}}_{[t-H,t]}$ and parameters $\hat{\mathbf{p}}$ are solution of the following optimization problem:

$$\min_{\hat{\mathbf{x}},\hat{\mathbf{p}}} \left\| \begin{bmatrix} \hat{\mathbf{x}}(t-H) \\ \hat{\mathbf{p}} \end{bmatrix} - \begin{bmatrix} \overline{\mathbf{x}}(t-H) \\ \overline{\mathbf{p}} \end{bmatrix} \right\|_S + \int_{t-H}^{t} \left(\|\mathbf{v}(\tau)\|_R^2 + \|\mathbf{w}(\tau)\|_Q^2 \right) d\tau$$

s.t. $\forall \tau \in [t-H, t]$,

$$\mathbf{v}(\tau) = \mathbf{y}(\tau) - h(\tau, \hat{\mathbf{x}}(\tau), \mathbf{u}(\tau), \hat{\mathbf{p}})$$
$$\mathbf{w}(\tau) = \dot{\hat{\mathbf{x}}}(\tau) - f(\tau, \hat{\mathbf{x}}(\tau), \mathbf{u}(\tau), \hat{\mathbf{p}})$$
$$\hat{\mathbf{x}}(\tau) \in \mathbb{X}$$
$$\hat{\mathbf{p}} \in \mathbb{P}$$

where $\overline{\mathbf{x}}(t-H)$ is a prior on the state estimation, $\overline{\mathbf{p}}$ is a prior on the estimated parameter. $\mathbb{X}$ is a set of acceptable values for the system's state and $\mathbb{P}$ is a set of acceptable values for the parameters. The notation $\|.\|_M$ denotes, for compatible sized vector $\mathbf{a}$ and matrix M, $\|\mathbf{a}\|_M = \sqrt{a^T M a}$.

MHE can be interpreted as a way to find the best state and parameter estimates given knowledge on the dynamics of the system, available measurements and prior knowledge. Common interpretation of the weighting matrices S, R and Q relate to covariances of gaussian signals. If measurement noise has covariance ν, state disturbance/model mismatch covariance η and estimation error has covariance π, we define:

$$R = \nu^{-1}, \qquad Q = \eta^{-1}, \qquad S = \pi^{-1}$$

[13], [14] provide a comprehensive overview of the methods to solve such problems, either through *indirect* (solve, then discretize) or *direct* methods (discretize, then solve). Most practical implementations rely on the direct method, as a plethora of tools is available thanks to the development of nonlinear programming (NLP) and since indirect methods often become intractable when the size of the problem increases.

A. Transcription of the problem into a non-linear program

The optimization problem of MHE is solved numerically with a time period T_s, using the data that is available on the interval $[t-H, t]$, where $H = NT_s$ with $N \in \mathbb{N}$. It is necessary to transcribe the infinite-sized optimization problem as a finite-sized NLP problem to be solved numerically. We discuss here some common methods of transcription for optimal control problems: single-shooting, multiple-shooting and direct-collocation.

1) Single and multiple-shooting: Single-shooting corresponds to a sequential transcription of the problem. The decision variables of the problem are discretized and the whole trajectory of the system is constructed in the "simulation step". This strategy can suffer from numerical instability and numerical integration of the system dynamics can be slow, which is why simultaneous transcription methods are preferred for optimal control problems.

One such simultaneous method is multiple-shooting, which introduces intermediate states on the trajectory as decision variables. For each interval $[t_k, t_{k+1}]$, a start node $x_{start}[t_k]$ and end node $x_{end}[t_{k+1}]$ are defined. Integration is defined on each subinterval with continuity constraints. The optimization problem then includes the following continuity constraints on the states:

$$x_{end}[t_{k+1}] = \Phi(x_{start}[t_k], u_k)$$
$$x_{end}[t_{k+1}] = x_{start}[t_{k+1}]$$

Where Φ is a discrete-time model of the system. The additionnal decision variables and constraints complexify the optimization problem but the resulting problem is sparser than single-shooting transcription. Exploiting the sparsity of a problem can help significantly speedup the resolution, which is achieved by solvers such as IPOPT [15]. Another advantage to multiple-shooting is numeric stability due to the enforcement of continuity constraints.

2) Direct collocation: Collocation methods in numerical integration refer to a class of implicit Runge-Kutta methods, which means that they are high-order one-step integration methods. Implicit methods are more stable than explicit methods and are thus suitable for the integration of stiff models. Choosing the Radau basis [13] with n points leads to an L-stable integration method of order $2n-1$, which is

desirable when dealing with stiff systems. A more comprehensive outlook on the theory, analysis and implementation of collocation methods in the context of optimal control can be found in [12]. The MHE implementation that we present is based on direct-collocation as it it suitable to deal with the stiff reactor core model and can deliver fast solutions of the optimization problem.

Direct-collocation transcription introduces the collocated states of the Runge-Kutta method in each integration interval $[t_i, t_{i+1}]$ as decision variables of the optimization problem. In the context of numerical integration, the intermediate points are discarded: the value of the solution at the end of the previous integration interval is the only quantity required for the current integration interval. In direct-collocation, since the collocated state are retained in the decision variables, they can also be used as the nodes of a gaussian quadrature in the evaluation of the cost function. For a s-order collocation method, the solution of the differential equation $\dot{\mathbf{x}}(t) = f(t, \mathbf{u}(t), \mathbf{x}(t), \mathbf{p})$ and the integrand of the cost function $F(x)$ are approximated on $[t_i, t_{i+1}]$ by the s-order polynomials $P(t)$ and $T(t)$. On each interval $[t_i, t_{i+1}]$ define s collocation nodes $t_{i,k} = t_i + h\tau_k, 0 \leq \tau_k \leq 1 \forall k = 1..s$ and corresponding decision variables $\mathbf{x}^{\mathrm{c}}_{i,k}$. Define the Lagrange polynomials:

$$\forall t \in [t_i, t_{i+1}], L_k(t) = \prod_{\substack{l=1 \\ l \neq k}}^{s} \frac{t - t_{i,l}}{t_{i,k} - t_{i,l}} \quad \text{such that} \quad L_k(t_{i,l}) = \delta_{k,l}$$

We construct the approximation polynomials of the solution and integrand of the cost function:

$$\forall t \in [t_i, t_{i+1}],\ P(t) = \sum_{k=1}^{s} L_k(t)\mathbf{x}^{\mathrm{c}}_{i,k},\ T(t) = \sum_{k=1}^{s} L_k(t) F\left(\mathbf{x}^{\mathrm{c}}_{i,k}\right)$$
$$\forall k = 1..s,\ P(t_{i,k}) = \mathbf{x}(t_{i,k}) = \mathbf{x}^{\mathrm{c}}_{i,k},\ T(t_{i,k}) = F(\mathbf{x}(t_{i,k})) = F(\mathbf{x}^{\mathrm{c}}_{i,k})$$

The approximated solution P corresponds with the exact solution of the differential equation at the collocation points, so $\forall k = 1..s$ we have the following constraints:

$$P'(t_{i,k}) = f(t_{i,k}, \mathbf{u}(t_{i,k}), \mathbf{x}^{\mathrm{c}}_{i,k}, \mathbf{p}) = \sum_{l=1}^{s} \underbrace{L'_l(t_{i,k})}_{a_{l,k}} \mathbf{x}^{\mathrm{c}}_{i,l}$$

At the end of the integration interval, we have:

$$\mathbf{x}_{i+1} = P(t_{i+1}) = \sum_{k=1}^{s} \underbrace{L_k(t_{i+1})}_{b_k} \mathbf{x}^{\mathrm{c}}_{i,k}$$

The approximate integrand T corresponds with F at the collocation points, and we write:

$$\int_{t_i}^{t_{i+1}} F(\mathbf{x}(\tau))d\tau \approx \int_{t_i}^{t_{i+1}} T(\tau)d\tau = \int_{t_i}^{t_{i+1}} \sum_{k=1}^{s} L_k(\tau) F\left(\mathbf{x}^{\mathrm{c}}_{i,k}\right) d\tau$$
$$= \sum_{k=1}^{s} \underbrace{\left(\int_{t_i}^{t_{i+1}} L_k(\tau)d\tau\right)}_{q_k} F\left(\mathbf{x}^{\mathrm{c}}_{i,k}\right)$$

Using the same choice of collocation nodes τ_k on all intervals and keeping all intervals of constant length Δt we apply the change of variable $\tau = \frac{t - t_i}{\Delta t}$ and rewrite $\forall l \in [\![1 \dots s]\!]$:

$$\forall \tau \in [0,1], \tilde{L}_k(\tau) = L(t_i + \Delta t\tau) = \prod_{\substack{l=1 \\ l \neq k}}^{s} \frac{\tau - \tau_k}{\tau_k - \tau_l}$$

$$\forall l \in [\![1 \dots s]\!],\ a_{l,k} = \frac{1}{\Delta t}\tilde{L}'_l(\tau_k),\ b_l = \tilde{L}_l(1),\ q_l = \Delta t \int_0^1 \tilde{L}_l(\tau)d\tau$$

Note that a collocation method is totally defined by the choice of collocation nodes $(\tau_k)_{k \in [\![1 \dots s]\!]}$ and order s as they define the Lagrange polynomials. The presented collocation scheme is called *integral form* since the interpolation polynomial P interpolates the states of the solution. Another common derivation uses the *differential form* when P interpolates the *time derivative* of the states of the solution.

Finally, the non-linear program associated with the optimization problem is rewritten as:

$$\min_{\hat{\mathbf{x}}, \hat{\mathbf{p}}} J = \left\| \begin{bmatrix} \hat{\mathbf{x}}_{k-N+1} \\ \hat{\mathbf{p}} \end{bmatrix} - \begin{bmatrix} \overline{\mathbf{x}} \\ \overline{\mathbf{p}} \end{bmatrix} \right\|_S + \sum_{i=k-N+1}^{k-1} \|\mathbf{w}_i\|_Q + \sum_{i=k-N+1}^{k} \sum_{l=1}^{s} q_l \left\|\mathbf{v}_{i,l}\right\|_R$$

$$\text{s.t.} \quad \forall i \in [\![k - N + 1, \dots, k]\!],$$
$$\mathbf{w}_i = \hat{\mathbf{x}}_{i+1} - \sum_{l=1}^{s} b_l \hat{\mathbf{x}}^{\mathrm{c}}_{i,l}$$
$$\forall l \in [\![1 \dots s]\!],$$
$$\mathbf{v}_{i,l} = \mathbf{y}(t_{i,l}) - h(t_{i,l}, \mathbf{u}(t_{i,l}), \hat{\mathbf{x}}^{\mathrm{c}}_{i,l}, \hat{\mathbf{p}})$$
$$\sum_{m=1}^{s} a_{l,m} \hat{\mathbf{x}}^{\mathrm{c}}_{i,m} = f(t_{i,l}, \mathbf{u}(t_{i,l}), \hat{\mathbf{x}}^{\mathrm{c}}_{i,l}, \hat{\mathbf{p}})$$
$$\hat{\mathbf{x}}^{\mathrm{c}}_{i,k} \in \mathbb{X}$$
$$\hat{\mathbf{p}} \in \mathbb{P}$$

An advantage of this approach over single and multiple-shooting is that it's a single-phase optimization problem. Due to the collocation constraints, no dedicated numerical integration phase is necessary: a feasible solution of the optimization problem is always a trajectory of the system. If we consider the highly sparse structure of the NLP problem and suitable solvers, the potential speedups offered by the technique make up for the overhead of introducing additional decision variables.

Lastly, there remains a caveat to this approach, which we discuss now. For a given choice of collocation nodes, it is unlikely that the sampling rate of the outputs and inputs match with the collocation nodes. Collocation nodes in the Radau and Legendre collocation scheme are not evenly distributed. A result of this formulation it is necessary to use interpolation to retrieve the value of the inputs and outputs of the system at the collocation nodes. It is compatible with complex plants in industrial settings: signals have to be read from a data bus shared across different systems and could be delayed, infrequent or dropped when managing bandwidth or due to prioritization of signals.

B. Extension of MHE to parameter estimation

Online estimation of parameters in the case of MHE can be implemented in different manners. The first option is to consider a single decision variable which is used in the relevant constraints of the optimization problem. The other option is to consider an augmented state of the system, which

contains the original state and the parameters to be estimated. In general, parameters are assumed to have a constant value over a given time period such as the estimation window, so we write $\dot{\mathbf{p}}_\mathbf{i} = 0,\ i = 1..m_p$. However, if some model of the evolution of the parameters over time is available it can be used instead. We will suppose in the rest of the paper that estimated parameters have a constant value over the estimation window of MHE. In this context, the augmented model becomes:

$$\begin{pmatrix}\dot{\mathbf{x}}(t)\\ \dot{\mathbf{p}}(t)\end{pmatrix} = \begin{pmatrix}f(t,\mathbf{u}(t),\mathbf{x}(t),\mathbf{p}(t))\\ \mathbf{0}_{m_p}\end{pmatrix}$$
$$\mathbf{y}(t) = h(t,\mathbf{u}(t),\mathbf{x}(t),\mathbf{p}(t))$$

where $\mathbf{0}_{m_p}$ is a zero vector of size m_p.

This formulation allows us to use any state estimation technique for parameter estmation without requiring to alter the implementation, as well as to model the evolution of parameters. On the other hand, we add many intermediate decision variables to the NLP, since all the values of $\mathbf{p}(t)$ at the collocation nodes have to be considered.

IV. Implementation and results

In previous work[3], we presented an implementation of a state estimator using generic tools available in the Matlab [16] programming environment, `fmincon` and `ode15s`. The resulting MHE scheme was straightforward to implement with minimal changes required on existing source code and presented satisfying performance for onsite use. Maintaining the same approach for simultaneous estimation of states and parameters was unsuccessful due to the increased problem complexity once adding parameters to be estimated. The presented implementation relies, for its part, on the CasADi[17] toolbox with the Matlab[16] interface. The optimization solver is IPOPT[15], which implements a state of the art primal-dual interior point method. It can be warmstarted to speed the solution of optimization problems up. The estimation horizon is H = 1h and the model is discretized using collocation of order 3 and a time-discretization T_s = 1min. Longer estimation window are necessary to increase sensitivity of the cost function to the parameters of xenon dynamics, as it has a long characteristic time.

Validation and analysis of the obtained performances is proposed through a comparison with an extended Kalman Filter under common tuning parameters. The EKF was also implemented using CasADi and its convenient differentiation interface. The model in the EKF is a discretization of the continuous dynamics using collocation of order 3 and sampling period of 1min. CasADi implements interpolation tables that can be differentiated and used with symbolic variables, which is an important element for the model which uses tabulated anti-reactivity values. System's inputs and measurements have to be interpolated at the collocation nodes. For both estimation algorithms, we implement parameter estimation through an augmented model, as outlined in section III-B. Additionally, we highlight the advantage of using MHE over EKF when dealing simultaneously with state and parameter estimation. This is achieved by increasing the state of the system as described in section III.B. The EKF is indeed able to reconstruct the state of the system alone, albeit with slower convergence than MHE, but fails to estimate the extended state. On the other hand, MHE handles parameter estimation with more success and without requiring a complete redesign or retuning of the estimator.

The validation of the implementation is carried by adding an error term to the true initial state of the system, sampled from a gaussian distribution corresponding to 20% relative error. Only approximated values of the parameters to be estimated are assumed to be available: they are initialized to the order of magnitude of their true value. The validation data was produced using $\Sigma_X = 5.5 \times 10^{-7}\text{s}^{-1}\%\text{PN}^{-1}$ and D = 860pcm. Therefore, the parameters are initialized to $\Sigma_X = 10^{-5}\text{s}^{-1}\%\text{PN}^{-1}$ and D = 1000pcm, such that initial errors are of 81% and 16% respectively. Finally, the code was run on a consumer grade laptop of with an `Intel®` Core™ i5-8365U CPU clocked at 1.6GHz and 16Gb of DDR4 RAM, running Microsoft Windows 10.

Both the EKF and MHE share common tuning parameters as outlined in section III. The initial covariance estimate of EKF is such that $P_0 = S^{-1/2}$, where S is the weighting matrix in the arrival cost term of MHE.

The implemented algorithm makes simplifying assumptions: the arrival cost is computed using a constant weighting matrix S and a perfect model is assumed (which is to say that the slack variables (w_k) are set to 0). Matrix R is chosen according to noise consideration on the measurements. Denoting I_n the unit matrix of dimension n and $0_{n,m}$ the zero matrix of size $n \times m$, the EKF covariance of the measurement noise and the process noise are given by $R^{-1/2}$ and $Q^{-1/2}$:

$$R^{-1/2} = \begin{bmatrix}0.5I_2 & 0_{2,6}\\ 0_{6,2} & 0.2I_6\end{bmatrix}\ Q^{-1/2} = \begin{bmatrix}0.1I_{21} & 0_{21,12}\\ 0_{12,21} & I_{12}\end{bmatrix}\ S^{-1/2} = I_{33}$$

Fig. 2 shows the relative estimation error for both parameters Σ_X and D using MHE and EKF. Since MHE estimates the entire estimation window each time the optimization problem is solved, we choose to represent the estimation at the beginning of the window. MHE proves to be well-suited for this task, as the final estimation error for the parameters is below 0.5% relative error, whereas the Kalman Filter converges to an erroneous estimation.

We interpret the discrepancy between estimators as a result of the stiffness of the model. Stiffness impacts the sensitivity of each estimator with respect to the estimated parameters. We can think of EKF as having an horizon of dt while MHE uses a sixty times longer horizon. Xenon has a slow dynamics when compared to the faster dynamics of the model. In this context, an error in Σ_X will have less impact on xenon over a shorter horizon.

As a result of the erronated parameter estimates, the state estimates produced by the Kalman filter are erroneous as well, especially for the case of xenon. Since neutron fluxes are measured, a wrong value for D has a lower impact on them. On the other hand, xenon is not directly measured and its production is a result of the decay of iodine, which is the result of the decay of the fuel. The estimation of xenon relies

on an accurate value for Σ_X.

On the other hand, Fig. 3 illustrates that state estimates produced by MHE are more accurate, with normalized relative errors of less than 1% thanks to the superior parameter estimation when compared to those obtained from the EKF. The introduction of constraints on state and parameter estimation does not affect the accuracy of the estimates, as the inequality constraints remain inactive. Including these conditions adds no overhead to the algorithm's execution time.

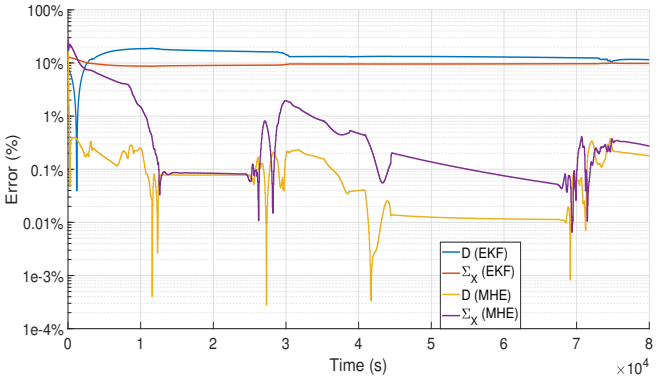

Fig. 2: Relative parameter estimation error for EKF and MHE (simultaneous estimation)

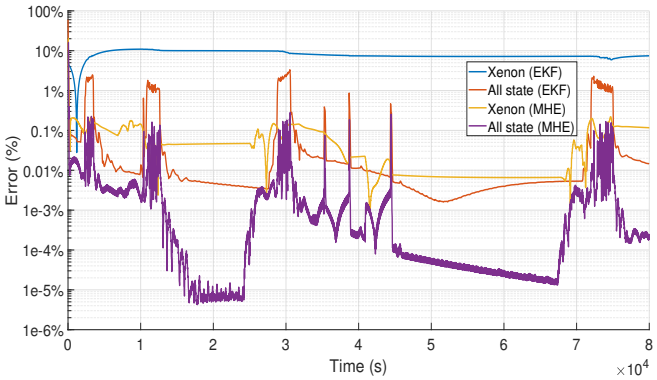

Fig. 3: Relative state estimation error for EKF and MHE (simultaneous estimation)

The improved accuracy of MHE for both state and parameter estimation does come at the price of an increased computational effort. Solving each MHE problem (therefore estimating a whole hour) took an average of 1.35s against 102ms for the EKF.

V. Conclusion and outlook

We have presented an implementation of Moving Horizon Estimation for the simultaneous estimation of state variables and selected parameters within a nuclear core model. This model, characterized by stiffness and strong nonlinearities in certain dynamics, posed significant challenges. We discussed the choice of direct collocation as a suitable method for transcribing the MHE optimization problem, emphasizing its advantages compared to other commonly employed techniques. By tailoring the nonlinear programming problem to the MHE requirements and solving it within a dynamic load-follow scenario, we demonstrated the efficacy of the solution proposed, intrinsically and by comparison. Indeed, Extended-Kalman Filter estimations were shown to fail to converge to the true states and parameters of the model. This research highlights the efficacy of MHE in enhancing state and parameter estimation within complex systems like PWRs, offering potential advancements in control and safety for nuclear power plants. Our forthcoming research will focus on implementing output Model Predictive Control, capitalizing on the presented estimation scheme.

References

[1] G. Dupré, A. Grossetête, P. Chevrel, and M. Yagoubi, "Enhanced Flexibility of PWRs (Mode A) Using an Efficient NMPC-Based Boration/Dilution System," in *2021 European Control Conference (ECC)*, pp. 1092–1098, June 2021.

[2] G. Dupré, P. Chevrel, M. Yagoubi, and A. Grossetete, "Design and Comparison of Two Advanced Core Control Systems for Flexible Operation of Pressurized Water Reactors," *Control Engineering Practice*, 2022. Publisher: Elsevier.

[3] L. Gruss, P. Chevrel, M. Yagoubi, M. Thieffry, and A. Grossetête, "Moving horizon estimation of xenon in pressurized water nuclear reactors using variable-step integration," in *2023 European Control Conference (ECC)*, pp. 1–6, June 2023.

[4] M. Soroush, "State and parameter estimations and their applications in process control," *Computers & Chemical Engineering*, vol. 23, pp. 229–245, Dec. 1998.

[5] M. H. Zahedi Ygane and G. R. Ansarifar, "Extended Kalman filter design to estimate the poisons concentrations in the P.W.R nuclear reactors based on the reactor power measurement," *Annals of Nuclear Energy*, vol. 101, pp. 576–585, Mar. 2017.

[6] S. R. Kumar and J. Devakumar, "Performance evaluation of neural network topologies for online state estimation and fault detection in pressurized water reactor," *Annals of Nuclear Energy*, vol. 175, p. 109235, Sept. 2022.

[7] A. Ponçot, J.-P. Argaud, B. Bouriquet, P. Erhard, S. Gratton, and O. Thual, "Variational assimilation for xenon dynamical forecasts in neutronic using advanced background error covariance matrix modelling," *Annals of Nuclear Energy*, vol. 60, pp. 39–50, Oct. 2013.

[8] A. Ponçot, *Assimilation de données pour la dynamique du xénon dans les cœurs de centrale nucléaire*. phd, Institut National Polytechnique de Toulouse, Oct. 2008.

[9] L. Meitner, F. Strassmann, and O. Hahn, "Künstliche Umwandlungsprozesse bei Bestrahlung des Thoriums mit Neutronen; Auftreten isomerer Reihen durch Abspaltung von -Strahlen," *Zeitschrift für Physik*, vol. 109, pp. 538–552, July 1938.

[10] F. Joliot, "Sur la rupture explosive des noyaux U et Th sous l'action des neutrons," *Journal de Physique et le Radium*, vol. 10, pp. 159–160, Mar. 1939.

[11] N. Metropolis and S. Ulam, "The Monte Carlo Method," *Journal of the American Statistical Association*, vol. 44, pp. 335–341, Sept. 1949.

[12] J. Rawlings, D. Mayne, and M. Diehl, *Model Predictive Control: Theory, Computation, and Design*, vol. 2. Nob Hill Publishing Madison, WI, 2017.

[13] A. Rao, "A Survey of Numerical Methods for Optimal Control," *Advances in the Astronautical Sciences*, vol. 135, Jan. 2010.

[14] L. T. Biegler, "An overview of simultaneous strategies for dynamic optimization," *Chemical Engineering and Processing: Process Intensification*, vol. 46, pp. 1043–1053, Nov. 2007.

[15] A. Wächter and L. T. Biegler, "On the implementation of an interior-point filter line-search algorithm for large-scale nonlinear programming," *Mathematical Programming*, vol. 106, pp. 25–57, Mar. 2006.

[16] MATLAB, *version 9.11.0 (R2021b)*. Natick, Massachusetts: The MathWorks Inc., 2021.

[17] J. A. E. Andersson, J. Gillis, G. Horn, J. B. Rawlings, and M. Diehl, "CasADi: a software framework for nonlinear optimization and optimal control," *Mathematical Programming Computation*, vol. 11, pp. 1–36, Mar. 2019.